# Trait repetitive negative thinking in depression is associated with functional connectivity in negative thinking state, not resting state

Masaya Misaki[a,b*], Aki Tsuchiyagaito[a,b], Salvador M. Guinjoan[a,c], Michael L. Rohan[a], Martin P. Paulus[a]

[a] Laureate Institute for Brain Research, Tulsa, OK, USA

[b] Oxley College of Health Sciences, The University of Tulsa, Tulsa, OK, USA

[c] Department of Psychiatry, Oklahoma University Health Sciences Center at Tulsa, Tulsa, OK, USA

## Abstract

Resting-state functional connectivity (RSFC) has been proposed as a potential indicator of repetitive negative thinking (RNT) in depression, while inconsistent findings have been reported. This study utilized connectome-based predictive modeling (CPM) to investigate whether RSFC and negative-thinking-state functional connectivity (NTFC) could predict RNT in individuals with Major Depressive Disorder (MDD). Although RSFC distinguished between healthy and depressed individuals, it did not predict trait RNT (as assessed by the Ruminative Responses Scale-Brooding subscale) in depressed individuals. Conversely, NTFC predicted trait RNT in depressed individuals with significant accuracy, but could not differentiate between healthy and depressed individuals. Connectome-wide analysis revealed that negative thinking in depression was associated with higher FC between default mode and executive control regions, which was not observed in RSFC. Our findings suggest that RNT in depression is associated with an active mental process involving multiple brain regions across functional networks that is not represented in the resting state.

## Introduction

Repetitive negative thinking (RNT) is defined as a perseverative thought process that focuses on one's problems or negative experiences in the present, past, and future (Ehring, 2021; Ehring and Watkins, 2008). Rumination and worry are the two main clinical types of RNT, with rumination referring to a passive, repetitive and evaluative focus on the symptoms of distress, whereas worry is a chain of thoughts focused on possible future negative outcomes (Nolen-Hoeksema et al., 2008). Rumination is often seen in individuals with Major Depressive Disorder (MDD) and has a moderate genetic correlation with MDD (Johnson et al., 2014). RNT predicts the onset of new episodes and the maintenance of existing symptoms of depression and is associated with reduced treatment response (Nolen-Hoeksema et al., 2008; Watkins and Roberts, 2020). The increased morbidity and treatment resistance of MDD individuals with RNT create a forceful impetus to identify the neurobiological underpinnings of RNT.

The neural correlates of RNT have been investigated using fMRI resting-state functional connectivity (RSFC), with the assumption that changes in the resting state may indicate intrinsic brain functional changes in depression (Hamilton et al., 2015; Zhang et al., 2021). Given that RNT involves the process of perseverative thinking of self-referential negative thoughts (Ehring, 2021), many studies have focused on the default mode network (DMN) areas that have been implicated in self-referential thinking (Hamilton et al., 2015). For example, increased RSFC in DMN regions has been frequently reported to be associated with high RNT in depression (Bessette et al., 2018; Hamilton et al., 2015; Jacob et al., 2020; Makovac et al., 2020; Misaki et al., 2020; Stern et al., 2022; Wise et al., 2017; Yang et al., 2022; Zhu et al., 2017). RNT has also been

associated with altered RSFC between the DMN and other regions, including the dorsolateral prefrontal cortex (Ichikawa et al., 2020; Peters et al., 2016), the amygdala (Connolly et al., 2013; Peters et al., 2016; Satyshur et al., 2018), and other executive control network nodes (Connolly et al., 2013; Feurer et al., 2021; Satyshur et al., 2018). However, in contrast to the RSFC findings of increased connectivity within the DMN and between the DMN and other regions, meta- and mega-analysis studies of large cohort data have reported decreased or no difference in DMN RSFC in depressed individuals (Goldstein-Piekarski et al., 2022; Tozzi et al., 2021; Yan et al., 2019; Zhang et al., 2020). Connectivity outside of the DMN (i.e., language and emotional salience regions) has also been suggested to differentiate individuals with high and low RNT (Tsuchiyagaito et al., 2022). Furthermore, rumination severity is not correlated with RSFC after controlling for other clinical measures of worry, whereas a worry-specific association was found after controlling for rumination (Andreescu et al., 2015), suggesting that RSFC is more closely associated with worry than rumination.

Recently, concerns have been raised about the functional implications of resting-state brain activation. Resting-state fMRI may not reflect the true resting state of the brain, but rather a state that is not constrained by a specific task (Finn, 2021; Gonzalez-Castillo et al., 2021) and can vary over time (Greene et al., 2018; Lurie et al., 2020). It has been argued that the assumption that resting-state fMRI reflects intrinsic brain function is inaccurate due to its temporal variability and the presence of the same network structure in both resting and task-active states (Finn, 2021). Several studies have also suggested that task-active states are more informative than the resting state in revealing the neurophysiological associations of individual cognitive traits (Finn and

Bandettini, 2021; Greene et al., 2020; Greene et al., 2018; McCormick et al., 2022). Therefore, it is possible that the brain functional changes associated with RNT in depression may be more prominent during a task state rather than during the resting state.

Indeed, task-based studies using a rumination-inducing task have also found differences in brain activity between high and low RNT individuals in depression. For example, a study focusing on the DMN found decreased connectivity within DMN subsystems during rumination (Chen et al., 2020). Functional changes related to RNT in a task-active state have also been observed in regions other than the DMN, including connectivity between the salience and anterior parietal networks (i.e., low connectivity between these networks was associated with high RNT following a sad event) (Lydon-Staley et al., 2019), the reward-related regions (i.e., ventral striatum response was positively correlated with rumination) (Erdman et al., 2020; Jones et al., 2017), and connectivity in the DMN and executive control regions (increased connectivity between the angular gyrus and the rostrolateral prefrontal cortex region was associated with high rumination) (Jones et al., 2017). These findings suggest that the rumination induction task engaged not only the DMN, but also regions of the salience and executive control networks that were not active during the resting state.

Although altered brain function associated with RNT in depression has been studied both at rest and during negative thinking (NT), it remains unclear which brain state better characterizes clinical RNT, and whether findings in these states reflect the same or independent functional changes. One could argue that functional changes during an NT task may better elucidate the pathology of depression because RNT is characterized

by a negative thinking style (Nolen-Hoeksema et al., 2008). However, asking participants to engage in negative thinking may reduce the differences in brain states between individuals with and without RNT, and the induced negative thinking may not reflect the trait RNT. As such, the sensitivity for detecting RNT-related changes in brain function may be lower in the NT state than in the resting state. In fact, previous resting-state studies have often assumed that RSFC changes in MDD may reflect frequent spontaneous rumination at rest (Bessette et al., 2018; Connolly et al., 2013; Feurer et al., 2021; Hamilton et al., 2015; Jacob et al., 2020; Lois and Wessa, 2016; Nejad et al., 2013; Satyshur et al., 2018; Zhang et al., 2020; Zhang et al., 2022; Zhu et al., 2017). If this assumption is true, then resting and NT states should show similar changes in FC in depressed individuals, and FC in both states may be indicative of the severity of RNT in depression. However, if the resting and NT states reflect separate functional changes in depression, we should consider the implications of each state separately and which state better reflects the clinical trait of RNT.

The present study aims to investigate whether the resting state or the NT state is more associated with trait RNT in depression, and whether their changes reflect the same or different pathology. To achieve these goals, we utilized connectome-based predictive modeling (CPM) (Shen et al., 2017) and connectome-wide association analysis (Shehzad et al., 2014). CPM is a machine learning approach used to create a predictive model of the brain-behavior relationship from whole-brain FC patterns. Multivariate predictive modeling approaches like CPM can overcome the small effect size problem of brain-behavior associations in mass-univariate analyses (Marek et al., 2022; Rosenberg and Finn, 2022) because they can aggregate univariate features to

improve both sensitivity and robustness (Finn and Rosenberg, 2021; Rosenberg and Finn, 2022; Taxali et al., 2021). We applied CPM to whole-brain functional connectivity patterns in the resting and NT states to (1) discriminate individuals with MDD from healthy controls (HC) and (2) predict individual differences in trait RNT score, as measured by the brooding subscale of the Ruminative Response Scale (RRS-B) (Nolen-Hoeksema and Morrow, 1991). By comparing CPM performance between the resting and NT states, we could examine which state was more informative for characterizing depression and trait RNT.

Furthermore, we adopted a connectome-wide association approach (Shehzad et al., 2014) using longitudinal multivariate distance matrix regression (MDMR) analysis (Misaki et al., 2018) to comprehensively investigate the FC changes in depression in both resting and NT states. MDMR (Anderson, 2001) is a multivariate analysis that examines brain-behavior associations in whole-brain FC patterns. This analysis provides a valuable complement to the CPM results, which only select FCs sufficient for better classification and prediction, potentially missing the comprehensive FC patterns associated with depression and RNT. In contrast, MDMR quantifies the entire connectivity associated with depression and RNT in the whole-brain voxel-to-voxel connectivity patterns. By combining these approaches, we assessed the functional implications of FC changes in MDD in both the resting and NT states and their association with individuals' RNT trait.

## METHODS

### Participants

Twenty-eight medically and psychiatrically healthy (HC) individuals and forty-two individuals with MDD participated in the study. Each participant performed resting and

rumination-inducing negative thinking (NT) tasks, which followed by other task runs including neurofeedback training (Tsuchiyagaito et al., 2023; Tsuchiyagaito et al., 2021). The present study analyzed their fMRI data during the resting-state and NT tasks. MDD participants met the DMS-5 (American Psychiatric Association, 2013) criteria for unipolar MDD based on the Mini-International Neuropsychiatric Interview 7.0.2 (Sheehan et al., 1998), and had current depressive symptoms with Montgomery-Åsberg Depression Rating Scale (MADRS) score > 6 (Montgomery and Åsberg, 1979). See Tsuchiyagaito et al. (2021) and Tsuchiyagaito et al. (2023) for detailed inclusion and exclusion criteria. The study protocols were approved by the Western Institutional Review Board, and all participants gave informed consent to participate in the study.

Two HC and six MDD participants were excluded from the analysis due to excessive head motion (more than 30% of time points (TR) censored with > 0.2 mm frame-wise displacement threshold in image processing) in either the resting or NT task. As a result, data from 26 HC participants (20 females, mean age = 23 years) and 36 MDD participants (28 females, mean age = 34 years) were included in the analysis. Supplemental Information (SI) Table S1 presents participant demographics and rumination and depression symptom scores.

**Scanning sessions and imaging parameters**

The scanning session began with an anatomical scan, followed by a 6m50s resting state session and a 6m50s rumination-inducing NT task. In the resting state session, participants were instructed to clear their minds and not think about anything in particular while looking at the cross sign on the screen. In the NT task, participants were instructed to think of a recent time when they felt rejected by someone who meant a lot

to them while looking at the cross sign on the screen. Participants completed these scans before any other task sessions so that no effect of other tasks confounded the resting state and NT sessions. Also, the resting state session always preceded the NT task so that no effect of the NT task was confounded with the resting state scan.

MRI scans were performed using a GE 3 Tesla MR750 Discovery scanner (GE Healthcare, Milwaukee WI, USA). The anatomical scan acquired a T1-weighted image with the MPRAGE sequence of TR/TE = 5/2 ms, SENSE acceleration R = 2, flip angle = 8, delay/inversion time TD/TI = 1400/725 ms, sampling bandwidth = 31.2 kHz, FOV = 240 x 192 mm, 124 axial slices, slice thickness = 1.2 mm, and scan time = 4 min 59 s. The resting and NT session functional scans acquired T2*-weighted images with a gradient echo planar sequence of TR/TE = 2000/25 ms, flip angle = 90, SENSE acceleration R = 2, acquisition matrix = 96 x 96, FOV/slice = 240/2.9 mm, and scan time = 6m50s (205 TRs).

**MRI image processing**

Analysis of Functional NeuroImages package (AFNI; http://afni.nimh.nih.gov/) (Cox, 1996) was used for MRI image processing. The same processing pipeline was used for both resting and NT state data. The first three volumes of functional images were excluded from the analysis. Processing included despiking, RETROICOR (Glover et al., 2000) and respiratory volume per time (Birn et al., 2008) physiological noise corrections, slice timing alignment, motion alignment, nonlinear warping to the MNI template brain with resampling to $2mm^3$ voxel volume using the ANTs (https://picsl.upenn.edu/software/ants/) (Avants et al., 2008), spatial smoothing with a 6mm-FWHM Gaussian kernel within the brain mask, and scaling of the signal to the

percent change relative to the mean in each voxel. General linear model (GLM) analysis was then applied with censoring volumes with > 0.2mm frame-wise displacement and regressors of Legendre polynomial models of slow signal fluctuations, 12 motion parameters (3 shifts, 3 rotations, and their temporal derivatives), three principal components of ventricular signals, and local white matter average signal (ANATICOR) (Jo et al., 2010). The residual of the GLM analysis was used as the processed fMRI data for the calculation of functional connectivity.

**Brain parcellation for functional connectivity matrix calculation**

The Shen 268-node atlas (Finn et al., 2015; Shen et al., 2013) was used to parcellate brain regions. We excluded 38 regions around the orbitofrontal, ventricles, and in the lower part of the brain from the analysis, because they were not covered by functional images or showed significant signal loss in many participants. The map of the excluded regions and their region indices in the Shen 268-node atlas are shown in SI Figure S1.

Functional connectivity between the 230 regions was calculated for the mean signals in the regions using Pearson's correlation followed by Fisher's z-transformation. The upper triangular part of the connectivity matrix, 26335 values, was the input for the connectome-based predictive modeling (CPM) analysis.

**Connectome-based Predictive Modeling (CPM)**

CPM analysis was performed for two separate tasks: classification of MDD and HC individuals and prediction of Ruminative Response Style Brooding subscale (RRS-B) scores. The effects of age, sex, and average motion (frame-wise displacement) were regressed and removed from the connectivity values in each RSFC and NTFC data. These covariate effects were also removed from RRS-B scores in the RRS-B prediction.

In the MDD-HC classification task, CPM constructed a prediction model by 1) selecting connectivity with a large absolute *t*-value for the difference between MDD and HC groups (the *t*-value threshold was a hyperparameter optimized by nested cross-validation), 2) summing the selected connectivity values for each positive and negative *t*-value in each participant, and 3) fitting a logistic regression model to classify MDD and HC individuals from the summed scores of positive and negative connectivities, respectively (Shen et al., 2017). Classification performance was assessed using the F1 score, a harmonic mean of precision and recall (2 x (precision x recall) / (precision + recall)).

In the RRS-B prediction task, connectivity with a high absolute Pearson's correlation (*r*) with the RRS-B score were selected at 2), and a linear regression model was fitted to predict the RRS-B scores at 3) in the procedure described above. The performance of RRS-B prediction was evaluated by Spearman's correlation between the true and predicted RRS-B scores. The RRS-B prediction was performed only for the MDD group because prediction for all participants, including both MDD and HC, could be confounded by significant group differences in RRS-B scores.

These classification and prediction performances were evaluated by 5-fold cross-validation, with participants divided into the training (80%) and test (20%) sets. The model hyperparameters, absolute *t*-value and absolute correlation thresholds for connectivity selection, were optimized in the nested 4-fold cross-validation within the training set (dividing the training set participants into the training [75%] and validation [25%] sets) with grid search for $t$ = 1.0 to 5.0 with 0.5 intervals for MDD-HC classification and $r$ = 0.1 to 0.5 with 0.05 intervals for RRS-B prediction. The entire

procedure of 5-fold cross-validation was repeated 100 times to assess the confidence interval of the predictive performance. The statistical significance of the predictive performance was evaluated using the permutation test by randomly permuting the output values 1000 times. In each permutation iteration, 5-fold cross-validation was repeated 20 times with different random splits, and the median value was taken to create a null distribution.

**Connectome-wide association analysis**

For a comprehensive functional connectivity investigation of the differences between rest and NT states, between HC and MDD, and the RRS-B association, we performed multivariate distance matrix regression (MDMR) analysis on whole-brain voxel-to-voxel connectivity (Shehzad et al., 2014). MDMR is a variant of MANOVA that uses nonparametric statistics (Anderson, 2001). The analysis computes connectivity maps for a seed voxel, and the distance matrix of the whole-brain connectivity maps across samples (i.e., participant x run) is used as the multivariate dependent variable for the linear model with multiple explanatory factors. These procedures are repeated for each voxel as a seed, and the regression statistic is assigned to the seed voxel.

The processed fMRI images were resampled into $4mm^3$ voxels, and the seed and its connectivity map were constrained in the gray matter voxels. The distance matrix between the resting-state and NT-state connectivity maps for all participants, calculated by Euclid distance, was the dependent variable in the MDMR. We used the longitudinal design introduced by Misaki et al. (2018) to account for the within-subject factor of resting and NT runs. The model included state (rest, NT), group (MDD, HC), RRS-B score, interactions of these three factors, age, sex, motion size (mean FD), and subject-

specific factor variables (Misaki et al., 2018; Winkler et al., 2014). The significance of the MDMR statistic of the pseudo-*F* value (Anderson, 2001) was assessed by permutation test with 10,000 repeats. The map was thresholded by voxel-wise $p < 0.001$ and family-wise error correction by cluster-extent $p < 0.05$. The cluster-extent threshold was also evaluated by permutation test.

The regions with a significant effect in the sum of the factors of interest (state [resting, NT], group [MDD, HC], RRS-B, and their interaction) were used for the post-hoc seed-based connectivity analysis. The post-hoc analysis was performed in the original image resolution. Seed regions were placed at peak locations of the significant cluster in the MDMR statistical map by extracting peak coordinates separated by at least 30mm in a cluster. The seed region was defined by a sphere of 6mm radius centered on the peak coordinates. The mean signal time course of the seed region was used as a reference signal to calculate connectivity with other voxels in the whole brain. For the statistical testing of the post hoc analysis, we used linear mixed effect (LME) model analysis with the same linear model specification as the MDMR, except that the subject factor was entered as a random effect on the intercept. We used the lme4 package (Bates et al., 2015) with the lmerTest package (Kuznetsova et al., 2017) in the R language and statistical computing (R Core Team, 2022) for the LME analysis.

We note that the post-hoc analysis was performed to elucidate the connectivity map associated with the MDMR result, and the MDMR is the test for the global connectivity pattern, not for individual voxel-wise connectivity. Therefore, we used a lenient voxel-wise threshold ($p < 0.05$) in the post-hoc evaluation to illustrate the global connectivity pattern for the seed with significant MDMR statistics. Nevertheless, we evaluated the

cluster size threshold with this voxel-wise threshold using cluster size simulation with 3dClustSim in AFNI (Cox et al., 2017), so the result complies with the corrected $p < 0.05$ threshold. The map of each contrast (i.e., MDD-HC in each state, rest-NT in each group, and RRS-B association in each group and state) was calculated using the R emmeans package (Lenth, 2022).

## Results

### CPM prediction of HC and MDD groups

Figure 1A shows the distributions of F1 scores for the MDD-HC classification over 100 iterations of 5-fold cross-validation with different random splits. The median F1 scores were 0.775 ($p < 0.001$) for the RSFC and 0.727 ($p = 0.327$) for the NTFC. The difference in performance between RSFC and NTFC tended to be significant ($p = 0.057$). Connectivity included in the prediction model is plotted on the glass brain (Fig. 1B) and with a circle plot (Fig. 1C). These plots show the connectivity selected more than 50% of the time in multiple (100 x 5) cross-validation iterations. The line color indicates the mean connectivity difference (z-value) between MDD and HC groups (warm color indicates higher connectivity for MDD). In Figure 1C, the network labels are adapted from Drysdale et al. (2017). Note that these maps are presented only to illustrate the FC patterns used by CPM as a whole, and not to evaluate the individual FC association with the classification. As CPM is a multivariate pattern analysis, it is not appropriate to evaluate individual FC associations independently. Therefore, we did not conduct a strict statistical test to evaluate the independent effect of each FC.

In the resting state, CPM classified participants as MDD based on high connectivity within visual cortex and cerebellar regions and their connectivity to DMN regions. In the

circle plot (Fig. 1C), the one cool-colored line (represented by the bilateral LIMB [default mode/limbic] connection) indicated the reduced functional connectivity between the bilateral subgenual anterior cingulate cortex (sgACC) regions in MDD compared to HC. In the NT state, the CPM used FCs in similar areas as in the resting state, while the number of FCs consistently selected across the cross-validation iterations was fewer than in the resting state (Figs. 1B and 1C).

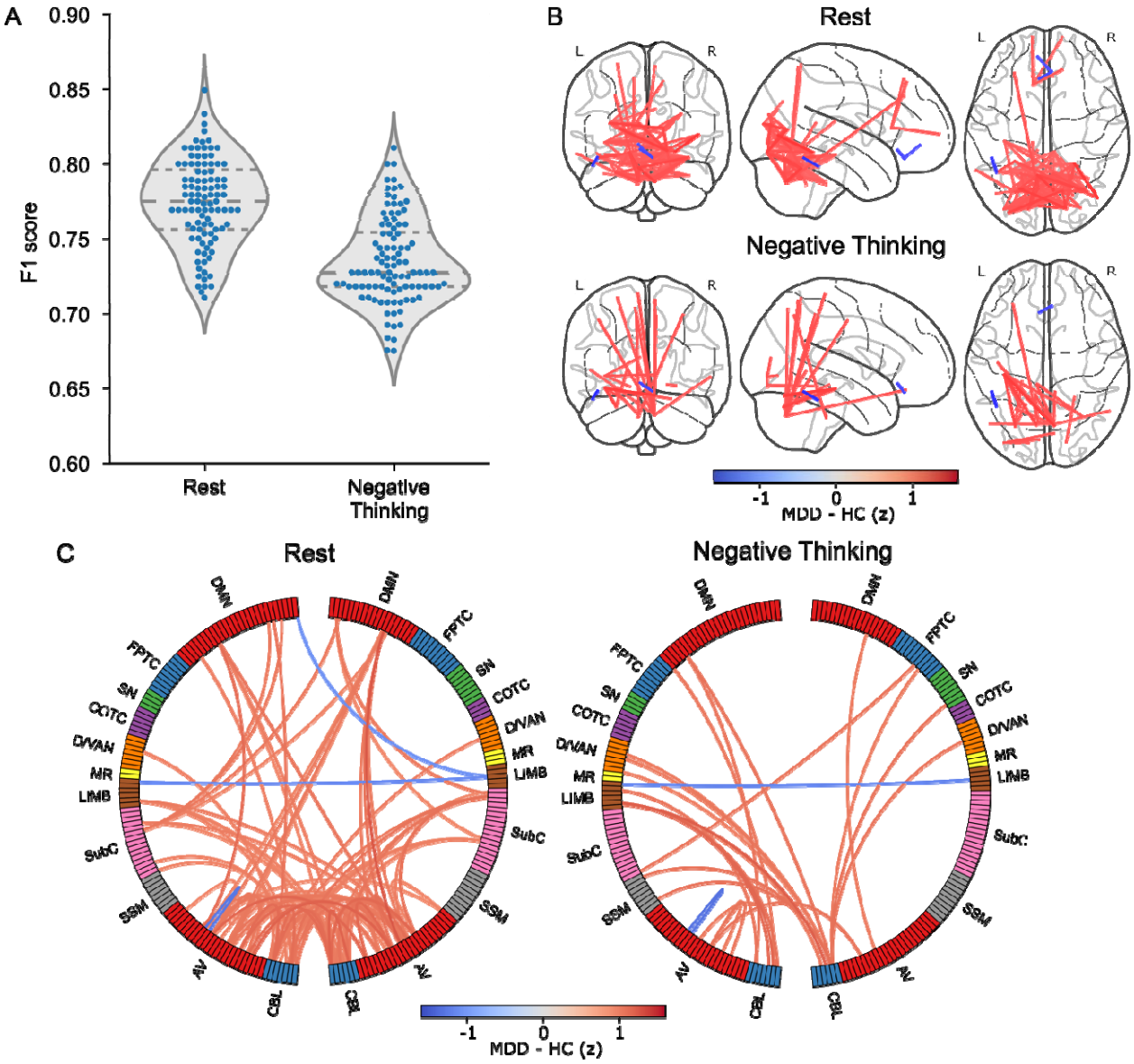

**Figure 1**. A. CPM prediction performance distributions for MDD-HC classification. Each point indicates one iteration of the 5-fold cross-validation result (100 iterations with different random splits were performed). The violin plot and horizontal lines indicate the distribution curve and quartile positions, respectively. B. Connectivity selected by the CPM model. The connectivities selected by more than 50% cross-validation iterations were plotted on the glass brain. The line color indicates the connectivity difference (z-value) between the MDD and HC groups. C. Circle plots of the same connectivities as in B summarized for each network region. Network labels are adapted from (Drysdale et al., 2017). DMN: Default Mode Network, FPTC: Fronto-Parietal Task Control, SN: Salience Network, COTC: Cingulo-Opperculum Task Control, D/VAN: Doral Visual Attention Network, MR: Memory Retrieval, LIMB: default mode/limbic, SubC: Subcortical, SSM: Sensory SomatoMotor, AV: Auditory-Visual, CBL: Cerebellum.

## CPM prediction of individual RRS-B score

Figure 2A displays the distributions of Spearman's correlations between true and predicted RRS-B scores for MDD over 100 iterations of 5-fold cross-validation with different random splits (SI Fig. S2 shows CPM prediction results including both groups). The median Spearman's correlations were -0.049 ($p$ = 0.447) for RSFC and 0.279 ($p$ = 0.041) for NTFC. The difference in performance between the resting and NT states was significant ($p$ = 0.043). Figures 2B and 2C show the connectivity included in the prediction model that was selected more than 85% of the time in the cross-validation iterations (plots with 50% threshold are shown in SI Fig. S3). Line color indicates FC correlation with RRS-B (z-transformed, warm color indicates positive correlation).

In the NT state, connectivity associated with RRS-B prediction was distributed over broad brain areas with high consistency across participants (across cross-validation). The higher connectivity from the thalamus regions (SubC nodes with dense, warm lines in Fig. 2C) in the NT state characterizes high RRS-B individuals in the MDD group. In

contrast, in the resting state, many connectivities consistently selected by CPM were negatively correlated with RRS-B (Fig. 2B and SI Fig. S3B).

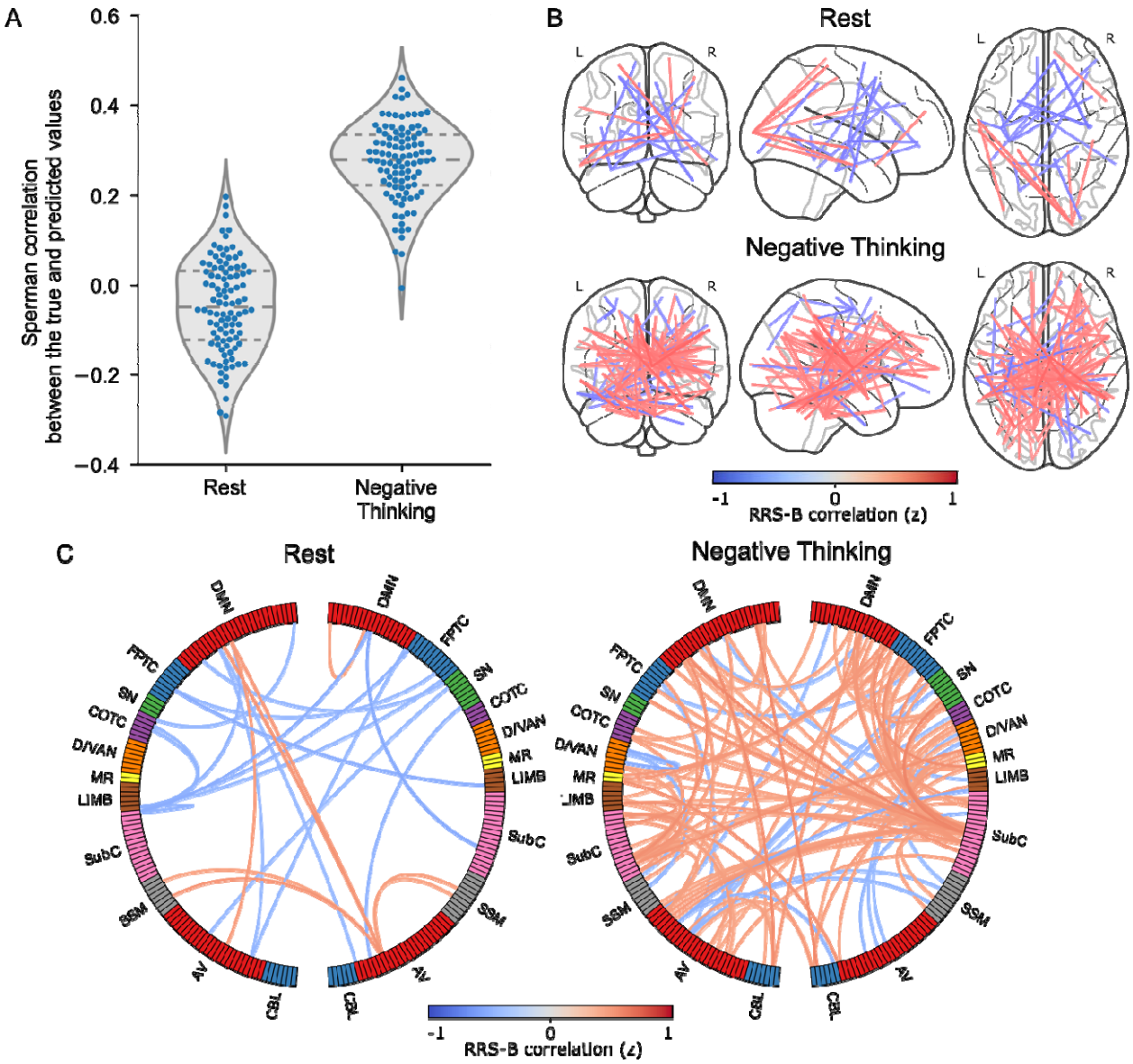


**Figure 2**. A. Distributions of the CPM prediction performance for individual RRS-B scores in the MDD group. Each point indicates one iteration of the 5-fold cross-validation result (100 iterations with different random splits were performed). The violin plot and horizontal lines indicate the distribution curve and quartile positions. B. Plots of the connectivity selected by the CPM model in more than 85% of the cross-validation iterations. Line color indicates the connectivity correlation with RRS-B (z-transformed). C. Circle plots of the same connectivities as in B,

summarized for each network region. Network labels are adapted from Drysdale et al. (2017) (see Fig. 1 for the network label abbreviations).

### MDMR connectome-wide association analysis

Figure 3 shows the regions with significant effects of interest (sum of the effects of state, group, RRS-B, and their interactions) with voxel-wise $p < 0.001$ and cluster-extent corrected $p < 0.05$ in the MDMR analysis. Significant clusters were found in DMN regions (i.e., precuneus, posterior cingulate cortex [PCC], medial prefrontal cortex [MPFC]), executive control regions (i.e., supplementary motor area [SMA] and lateral frontal regions including inferior frontal gyrus [IFG]), the caudate region, and the cerebellum. Post-hoc seed-based connectivity analysis was performed on the peak areas in these significant clusters. Table 1 shows the seed points used for the post-hoc analysis.

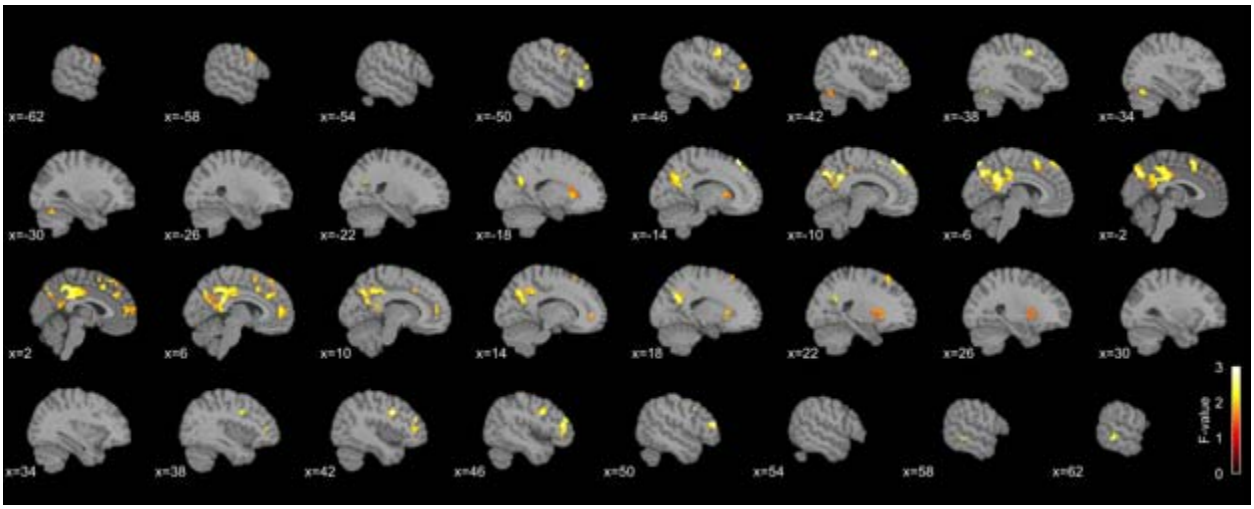


**Figure 3**. Significant regions with the MDMR statistics for the sum of the effects of interest (state, group, RRS-B, and their interactions) with voxel-wise $p < 0.001$ and cluster-extent corrected $p < 0.05$.

**Table 1**. The seed points in the significant clusters of the MDMR statistics.

| Seed index | x | y | z | Peak F-value | Area |
|---|---|---|---|---|---|
| 1 | -6 | -78 | 56 | 3.036 | Left Precuneus |
| 2 | 6 | -42 | 24 | 2.825 | Right Posterior Cingulate Cortex (PCC) |
| 3 | -2 | 14 | 56 | 2.664 | Left Supplementary Motor Area (SMA) |
| 4 | 6 | 50 | 8 | 2.53 | Right Medial Prefrontal Cortex (MPFC) |
| 5 | 50 | 38 | 12 | 2.714 | Right Inferior Frontal Gyrus (IFG) |
| 6 | 18 | 18 | 4 | 2.067 | Right Caudate |
| 7 | -46 | 6 | 44 | 2.811 | Left Middle Frontal Gyrus |
| 8 | -10 | 38 | 56 | 3.12 | Left Superior Frontal Gyrus |
| 9 | 42 | 6 | 36 | 3.082 | Right Inferior Frontal Gyrus (IFG) |
| 10 | -18 | 18 | 4 | 2.143 | Left Caudate |
| 11 | -34 | -66 | -24 | 2.322 | Left cerebellum (Crus I) |
| 12 | 6 | 34 | 32 | 2.249 | Right Cingulate Gyrus |
| 13 | 62 | -42 | -8 | 2.445 | Right Middle Temporal Gyrus |
| 14 | -50 | 34 | -8 | 2.488 | Left Inferior Frontal Gyrus |
| 15 | 22 | 26 | 60 | 2.098 | Right Superior Frontal Gyrus |
| 16 | 2 | 26 | 56 | 2.056 | Right Superior Frontal Gyrus |
| 17 | -50 | 42 | 16 | 2.203 | Left Inferior Frontal Gyrus |
| 18 | -58 | 6 | 40 | 1.968 | Left Middle Frontal Gyrus |

Figure 4 summarizes the representative MDD-HC contrast in the post-hoc analysis for the two seeds at the DMN hub nodes; PCC (seed 2; seed index corresponds to Table 1) and MPFC (seed 4). Significant FC maps of all seeds are shown in SI Figures S4 and S5 for the resting and NT states, respectively. In the resting state, MDD had higher connectivity than HC from these DMN seeds to the visual cortex regions (Figs. 4A and 4B). Other seeds also showed higher connectivity for MDD than HC in the occipital areas (SI Fig. S4), which was consistent with the CPM results. In the NT state, higher connectivity was also seen in the occipital regions (Figs. 4C and 4D), although the lower connectivity areas for MDD than HC of these seeds seen in the resting state (cool color regions in Figs. 4A and 4B) were not seen in the NT state (Figs. 4C and 4D), indicating that the MDD-HC contrast decreased in the NT state compared to the resting state. Notably, PCC seed connectivity in the precuneus regions was higher for HC than

MDD in the resting state (cool color regions in Figs. 4A), indicating that posterior DMN FC was higher for HC than MDD in the resting state. In addition, MDD group had higher connectivity between these DMN seeds and the IFG region in the NT state (Figs. 4C and 4D), which was not seen in the resting state.

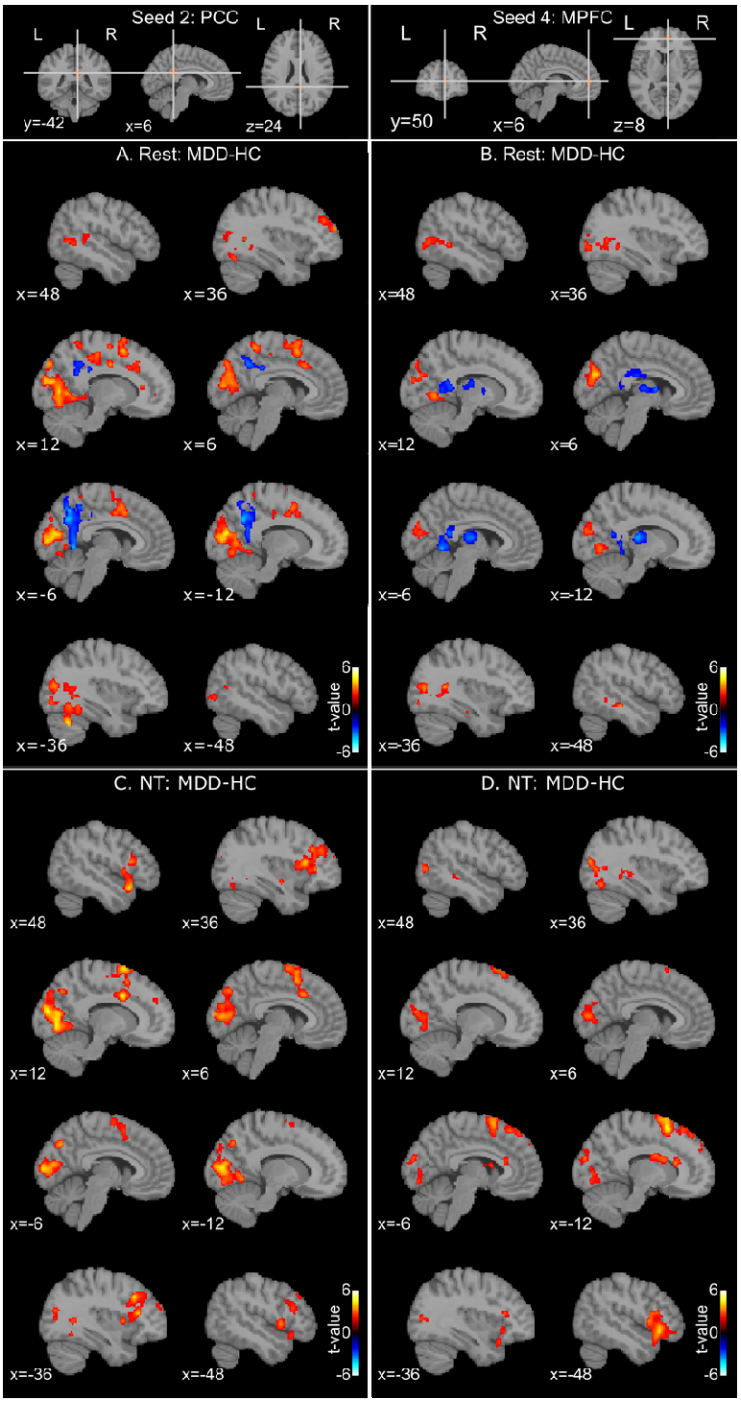

**Figure 4**. MDD-HC contrast connectivity maps in the MDMR post-hoc analysis with the PCC (seed 2) and MPFC (seed 4) seeds (top row) for the resting (A, B) and negative-thinking (NT; C, D) states. The map shows the *t*-value for the MDD-HC contrast. The seed index corresponds to Table 1. PCC: posterior cingulate cortex, MPFC: medial prefrontal cortex.

Figure 5 summarizes the representative NT-Rest contrast in the post-hoc analysis for three seeds, PCC (seed 2), SMA (seed 3), and right IFG (seed 9). Significant FC maps of all seeds are shown in SI Figures S6 and S7 for HC and MDD, respectively. The PCC seed, a DMN hub region, had higher connectivity with regions in the executive control areas, including the lateral premotor and prefrontal regions, and the anterior insula in the NT state than in the resting state in MDD (Fig. 5D). The SMA and IFG seeds had higher connectivity with the precuneus area in the NT state than in the resting state in MDD (Figs. 5E and 5F). These indicate that connectivity between posterior DMN regions (precuneus and PCC) and executive control regions was increased in the NT state in MDD. This increased connectivity was not observed in HC (Figs. 5A, 5B and 5C). Connectivity between the SMA and precuneus showed an opposite pattern between HC and MDD (Figs. 5B and 5E); it was higher in rest than in NT for HC, but higher in NT than in rest for MDD. Connectivity within the posterior DMN regions was higher in the resting state than in the NT state in both HC and MDD (Figs. 5A and 5D).

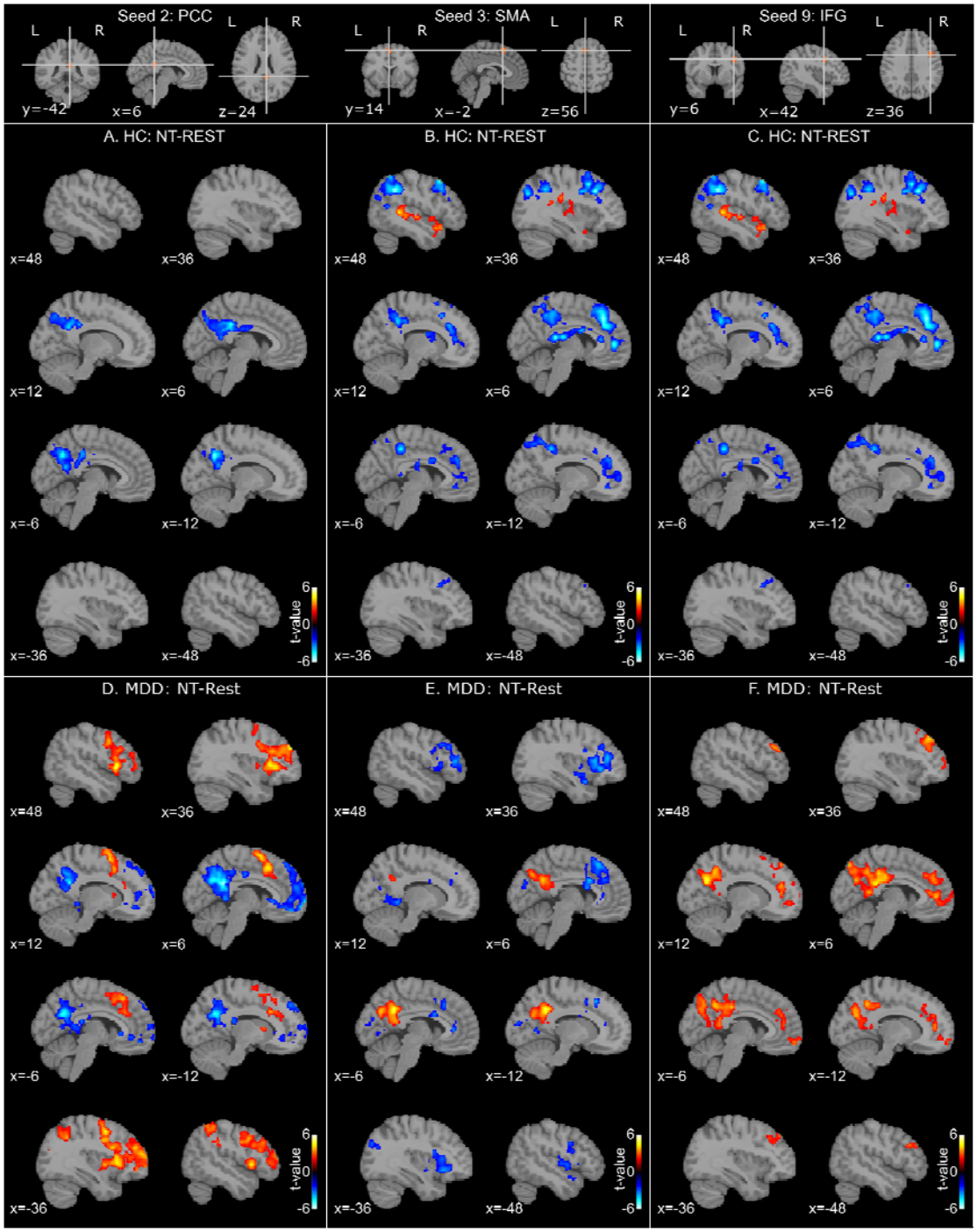


**Figure 5**. NT (negative thinking)-Rest contrast connectivity maps in the MDMR post-hoc analysis with the PCC (seed 2), SMA (seed 3), and right IFG (seed 9) seeds (top row) for the HC (A, B, C) and MDD (D, E, F) groups. The map shows the *t*-value for the NT-Rest contrast. The seed index corresponds to Table 1. PCC: posterior cingulate cortex, SMA: supplementary motor area, IFG: inferior frontal gyrus.

Figure 6 shows the RRS-B associations in the post hoc analysis for MDD. Significant FC maps of all seeds are shown in SI Figs. S8 and S9 for resting and NT states, respectively. We did not examine the RRS-B association in HC because the score in HC did not have enough variance to assess the association robustly. The most striking observation was the connectivity of the cerebellum (seed 11). In the NT state, the connectivity of this cerebellar seed showed a positive correlation with the RRS-B in broad cortical areas, including DMN regions (i.e., PCC and MPFC, Fig, 6D). In contrast, in the resting state, cerebellar connectivity associated with the RRS-B was restricted to motor and premotor cortex and did not extend to the DMN (Fig. 6B). The negative RRS-B association with the FC between the precuneus and thalamus was also observed for the resting state in MDD (Fig 6A).

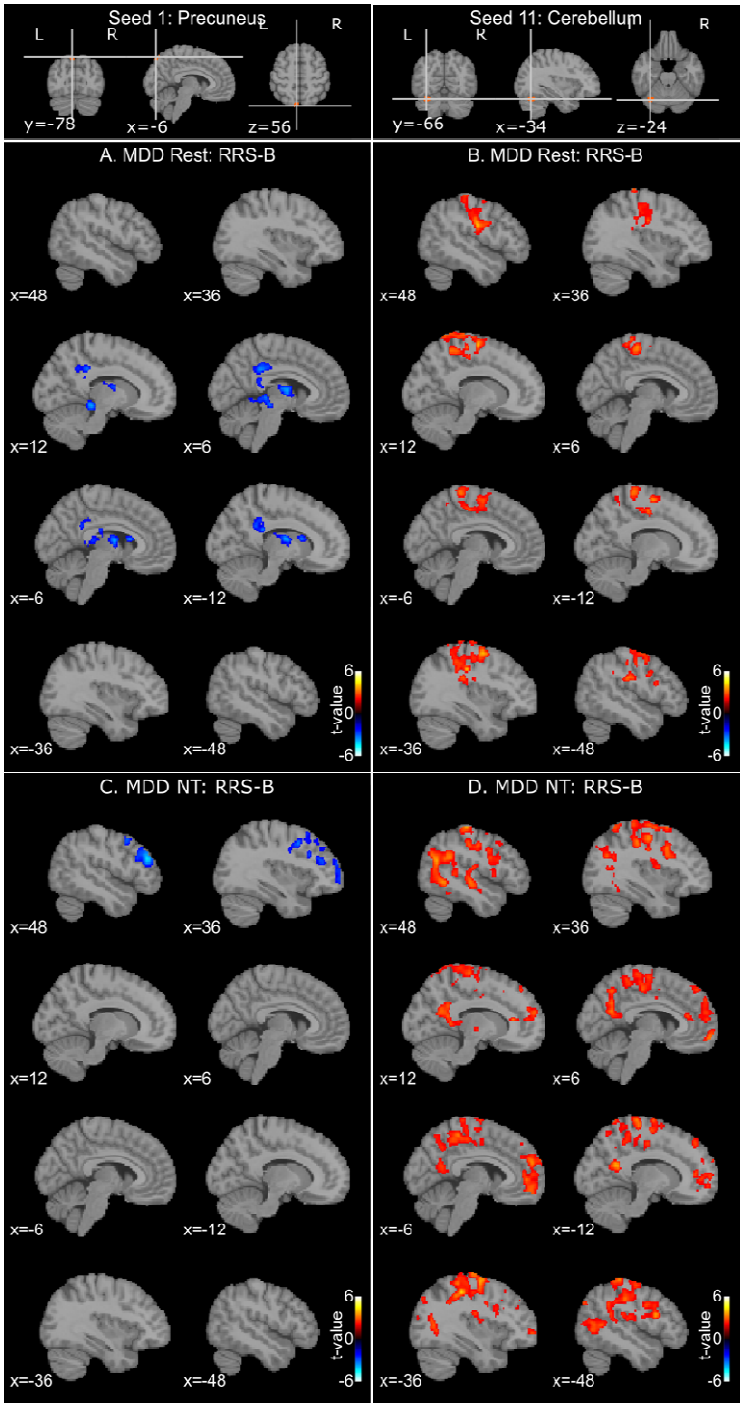


**Figure 6**. RRS-B association connectivity maps in the MDMR post-hoc analysis for seeds with the significant RRS-B association in the MDD group for the resting (A, B) and negative-thinking (NT; C, D) states. The map shows the *t*-value for the RRS-B association. The seed index corresponds to Table 1.

## Discussion

The primary findings of the present study are as follows: 1) CPM analysis demonstrated that RSFC was capable of distinguishing between HC and MDD individuals, but unable to predict trait RNT in depressed individuals. Conversely, 2) NTFC was capable of predicting trait RNT in depressed individuals, but unable to differentiate between HC and MDD individuals. The inability of NTFC to differentiate between HC and MDD individuals may be accounted for by the reduced difference in FC patterns between the groups when they were placed in a similar mental state with the NT task. As RSFC was more sensitive in distinguishing MDD from HC, investigating functional brain changes in MDD using resting state should be warranted. However, RSFC did not predict trait RNT in depression, suggesting that RSFC changes in depression do not reflect RNT. This finding contradicts the assumption that modifications in RSFC in MDD arise from heightened spontaneous rumination during the resting state in these individuals. While RSFC indicates changes in brain function in depression, such changes may be distinct from the RNT process.

Investigations of FC patterns associated with CPM prediction and complementary connectome-wide MDMR analysis further revealed the significant difference between resting and NT states in depressed individuals. In the MDD-HC CPM classification, more FCs were consistently selected in the resting state than in the NT state across between-subjects cross-validation splits, and in the MDMR, more seed regions showed a significant MDD-HC difference in the resting state than in the NT state (SI Figs. S4 and S5). This is consistent with the fact that CPM could classify FC patterns between healthy and depressed individuals with greater sensitivity in the resting state than in the

NT state. FCs distinguishing MDD from HC were found in areas of the visual cortex and cerebellum and their connections with DMN regions in both CPM and MDMR analyses. Reduced FC between bilateral sgACC areas was also used by CPM to classify MDD. Altered sgACC function in depression has been reported for MDD (Brakowski et al., 2017; Drevets et al., 2008), and disrupted sgACC activity could reduce its bilateral functional coupling. While increased visual cortex activation during rumination has been reported in adolescents with remitted MDD (Burkhouse et al., 2017), a negative correlation between a trait rumination score (RRS) and visual cortex activation in both resting and task (face classification) conditions has also been reported (Piguet et al., 2014). Thus, while the increased FC in visual cortex in MDD may at least reflect higher visual imagery than HC at rest, it may not be specifically associated with negative thinking.

Interestingly, DMN connectivity was not selected in the CPM classification, and MDMR analysis revealed decreased posterior DMN connectivity in MDD compared to HC in the resting state. This is consistent with the meta- and mega-analysis studies of large cohort data that reported decreased or no difference in resting-state DMN FC in depressed individuals (Goldstein-Piekarski et al., 2022; Tozzi et al., 2021; Yan et al., 2019; Zhang et al., 2020). These studies argued that the increased resting-state DMN FC reported in previous studies may include the inflated effect size due to small sample size (Marek et al., 2022), and the true effect size of the difference in resting-state DMN FC could be small.

In contrast to the MDD-HC classification, RRS-B prediction was well performed with NTFC, but not with RSFC. The FCs that were informative for predicting RRS-B in MDD

in the CPM analysis were distributed over large areas of the brain (SI Fig. S3). The involvement of many cortical regions, including the limbic and medial and dorsolateral prefrontal regions, has also been reported in the rumination induction task (Cooney et al., 2010). These suggest that RNT is associated with large-scale network and inter-network interactions (Lydon-Staley et al., 2019; Zhang et al., 2020) rather than a focal processing abnormality. MDMR results showing significant FC differences between resting and NT states in MDD support the perspective of multi-network involvement in the RNT process. Connectivity between the precuneus and executive control regions (i.e., SMA, IFG) and the salience network region (i.e., anterior insula) was increased in the NT state compared to the resting state in MDD participants (Fig. 5). Also, the FC between the DMN seeds and IFG in the NT state was significantly higher in MDD than in HC (Figs. 4C and 4D), suggesting that such an increase in the NT state is specific to depressed individuals.

When we used a strict threshold for plotting the FCs informative for predicting RRS-B, the dense connection was seen in the right thalamus area, which had a positive correlation with RRS-B (Fig. 2C). The significant RRS-B association with FC between thalamus and precuneus was also observed in the resting state in MDD (Fig. 6A), but in a negative direction, highlighting that the resting state in MDD had a significantly different FC pattern than the NT state. The involvement of the thalamus in RNT has been demonstrated in a 7T fMRI study (Steward et al., 2022), suggesting that the thalamus, with its extensive cortical pathways, may act to increase synchrony between cortical regions to maintain complex mental representations, including RNT. In addition, emerging clinical evidence suggests a role for right thalamic-cortical circuitry in the

amelioration of depression in neuromodulation treatments (Lippitz et al., 1999; Riestra et al., 2011; Scangos et al., 2021), highlighting the potential clinical implications of this particular finding to help refine neuromodulatory procedures for MDD.

The RRS-B association in the MDMR analysis was seen for the cerebellum seed connectivity with broad cortical regions. This cerebellar region (crus I) is functionally related to executive control network areas (Habas et al., 2009). A report of a blunted response of this region to reward anticipation in depressed individuals with high RNT (Park et al., 2022) also suggests that trait RNT may influence activation of this region. The associations of RRS-B with this seed to broad cortical regions, not limited to the executive control region but including the DMN regions in the NT state, suggest that the RNT is an active process involving multiple networks, not limited to the DMN. The increased FC between the SMA, a region that monitors and evaluates an active process (Bonini et al., 2014), and the precuneus, a region involved in self-referential thinking (Fig. 5E), also supports the idea that RNT in depression is an active process. The involvement of many cortical areas in the RNT process has also been reported in previous studies, including increased FC from the PCC to many cortical areas in the NT state compared to the resting state (Berman et al., 2014).

Discussing the limitations of the current study is warranted. The significant age difference between the MDD and HC groups may have biased the present results concerning the MDD-HC difference. To mitigate this, we excluded the age effect from the FCs in the CPM analysis, and age was included as a covariate factor in the MDMR analysis. However, excluding the age effect may have also removed the association between FC and depression if it interacted with age. Indeed, Andreescu et al. (2014)

found an interaction between age and anxiety on DMN connectivity, where the effect of anxiety on FC was greater in older participants. Therefore, we acknowledge that the present findings of FCs associated with MDD (MDD-HC contrast) may not be comprehensive, as age-interacted FC associations may have been missed. Nonetheless, the prediction of RRS-B was made only for MDD, and age differences between groups did not affect this prediction. Another limitation is that we focused on the rumination portion of the RNT in MDD, neglecting the association with worry, another form of RNT that has been extensively discussed in anxiety disorders. Thus, the current FC findings concerning trait RNT are limited to rumination aspects in MDD.

In conclusion, while resting state is often considered a proxy for ruminative state in individuals with depression, the present results showed that resting state is not similar to negative thinking and does not reflect trait RNT in MDD. Resting state, as an experimental procedure, does not necessarily reflect intrinsic functional activations (Finn, 2021), and the functional implications of resting state cannot be clarified without obtaining participants' introspective reports (Gonzalez-Castillo et al., 2021). Although the resting state may indicate abnormal brain activity in MDD, it may not reflect rumination. Negative thinking in depression is a more active process than in the resting state, involving interactions across multiple functional networks and not localized to a specific brain network.

## Acknowledgments

This work has been supported by The Laureate Institute for Brain Research and the National Institute of General Medical Sciences Center Grant Award Number (1P20GM121312). The content is solely the responsibility of the authors and does not necessarily represent the official views of the National Institutes of Health.

## References

American Psychiatric Association, 2013. Diagnostic and statistical manual of mental disorders (DSM-5). American Psychiatric Pub.

Anderson, M.J., 2001. A new method for non‐parametric multivariate analysis of variance. Austral ecology 26, 32-46.

Andreescu, C., Mennin, D., Tudorascu, D., Sheu, L.K., Walker, S., Banihashemi, L., Aizenstein, H., 2015. The many faces of anxiety-neurobiological correlates of anxiety phenotypes. Psychiatry Res 234, 96-105.

Andreescu, C., Sheu, L.K., Tudorascu, D., Walker, S., Aizenstein, H., 2014. The ages of anxiety--differences across the lifespan in the default mode network functional connectivity in generalized anxiety disorder. Int J Geriatr Psychiatry 29, 704-712.

Avants, B.B., Epstein, C.L., Grossman, M., Gee, J.C., 2008. Symmetric diffeomorphic image registration with cross-correlation: evaluating automated labeling of elderly and neurodegenerative brain. Med. Image Anal 12, 26-41.

Bates, D., Maechler, M., Bolker, B., Walker, S., 2015. Fitting Linear Mixed-Effects Models Using lme4. Journal of Statistical Software 67, 1–48.

Berman, M.G., Misic, B., Buschkuehl, M., Kross, E., Deldin, P.J., Peltier, S., Churchill, N.W., Jaeggi, S.M., Vakorin, V., McIntosh, A.R., Jonides, J., 2014. Does resting-state connectivity reflect depressive rumination? A tale of two analyses. Neuroimage 103, 267-279.

Bessette, K.L., Jenkins, L.M., Skerrett, K.A., Gowins, J.R., DelDonno, S.R., Zubieta, J.K., McInnis, M.G., Jacobs, R.H., Ajilore, O., Langenecker, S.A., 2018. Reliability, Convergent Validity and Time Invariance of Default Mode Network Deviations in Early Adult Major Depressive Disorder. Front Psychiatry 9, 244.

Birn, R.M., Smith, M.A., Jones, T.B., Bandettini, P.A., 2008. The respiration response function: the temporal dynamics of fMRI signal fluctuations related to changes in respiration. Neuroimage 40, 644-654.

Bonini, F., Burle, B., Liegeois-Chauvel, C., Regis, J., Chauvel, P., Vidal, F., 2014. Action monitoring and medial frontal cortex: leading role of supplementary motor area. Science 343, 888-891.

Brakowski, J., Spinelli, S., Dörig, N., Bosch, O.G., Manoliu, A., Holtforth, M.G., Seifritz, E., 2017. Resting state brain network function in major depression – Depression symptomatology, antidepressant treatment effects, future research. J Psychiatr Res 92, 147-159.

Burkhouse, K.L., Jacobs, R.H., Peters, A.T., Ajilore, O., Watkins, E.R., Langenecker, S.A., 2017. Neural correlates of rumination in adolescents with remitted major depressive disorder and healthy controls. Cogn Affect Behav Neurosci 17, 394-405.

Chen, X., Chen, N.X., Shen, Y.Q., Li, H.X., Li, L., Lu, B., Zhu, Z.C., Fan, Z., Yan, C.G., 2020. The subsystem mechanism of default mode network underlying rumination: A reproducible neuroimaging study. Neuroimage 221, 117185.

Connolly, C.G., Wu, J., Ho, T.C., Hoeft, F., Wolkowitz, O., Eisendrath, S., Frank, G., Hendren, R., Max, J.E., Paulus, M.P., Tapert, S.F., Banerjee, D., Simmons, A.N., Yang, T.T., 2013. Resting-state functional connectivity of subgenual anterior cingulate cortex in depressed adolescents. Biol Psychiatry 74, 898-907.

Cooney, R.E., Joormann, J., Eugene, F., Dennis, E.L., Gotlib, I.H., 2010. Neural correlates of rumination in depression. Cogn Affect Behav Neurosci 10, 470-478.

Cox, R.W., 1996. AFNI: software for analysis and visualization of functional magnetic resonance neuroimages. Comput Biomed Res 29, 162-173.

Cox, R.W., Chen, G., Glen, D.R., Reynolds, R.C., Taylor, P.A., 2017. FMRI Clustering in AFNI: False-Positive Rates Redux. Brain Connect 7, 152-171.

Drevets, W.C., Savitz, J., Trimble, M., 2008. The subgenual anterior cingulate cortex in mood disorders. CNS Spectr 13, 663-681.

Drysdale, A.T., Grosenick, L., Downar, J., Dunlop, K., Mansouri, F., Meng, Y., Fetcho, R.N., Zebley, B., Oathes, D.J., Etkin, A., Schatzberg, A.F., Sudheimer, K., Keller, J., Mayberg, H.S., Gunning, F.M., Alexopoulos, G.S., Fox, M.D., Pascual-Leone, A., Voss, H.U., Casey, B.J., Dubin, M.J., Liston, C., 2017. Resting-state connectivity biomarkers define neurophysiological subtypes of depression. Nat Med 23, 28-38.

Ehring, T., 2021. Thinking too much: rumination and psychopathology. World Psychiatry 20, 441-442.

Ehring, T., Watkins, E.R., 2008. Repetitive negative thinking as a transdiagnostic process. International Journal of Cognitive Therapy 1, 192-205.

Erdman, A., Abend, R., Jalon, I., Artzi, M., Gazit, T., Avirame, K., Ais, E.D., Levokovitz, H., Gilboa-Schechtman, E., Hendler, T., Harel, E.V., 2020. Ruminative Tendency Relates to Ventral Striatum Functionality: Evidence From Task and Resting-State fMRI. Front Psychiatry 11, 67.

Feurer, C., Jimmy, J., Chang, F., Langenecker, S.A., Phan, K.L., Ajilore, O., Klumpp, H., 2021. Resting state functional connectivity correlates of rumination and worry in internalizing psychopathologies. Depress Anxiety 38, 488-497.

Finn, E.S., 2021. Is it time to put rest to rest? Trends Cogn Sci 25, 1021-1032.

Finn, E.S., Bandettini, P.A., 2021. Movie-watching outperforms rest for functional connectivity-based prediction of behavior. Neuroimage 235, 117963.

Finn, E.S., Rosenberg, M.D., 2021. Beyond fingerprinting: Choosing predictive connectomes over reliable connectomes. Neuroimage 239, 118254.

Finn, E.S., Shen, X., Scheinost, D., Rosenberg, M.D., Huang, J., Chun, M.M., Papademetris, X., Constable, R.T., 2015. Functional connectome fingerprinting: identifying individuals using patterns of brain connectivity. Nat Neurosci 18, 1664-1671.

Glover, G.H., Li, T.Q., Ress, D., 2000. Image-based method for retrospective correction of physiological motion effects in fMRI: RETROICOR. Magn Reson Med 44, 162-167.

Goldstein-Piekarski, A.N., Ball, T.M., Samara, Z., Staveland, B.R., Keller, A.S., Fleming, S.L., Grisanzio, K.A., Holt-Gosselin, B., Stetz, P., Ma, J., Williams, L.M., 2022. Mapping Neural Circuit Biotypes to Symptoms and Behavioral Dimensions of Depression and Anxiety. Biol Psychiatry 91, 561-571.

Gonzalez-Castillo, J., Kam, J.W.Y., Hoy, C.W., Bandettini, P.A., 2021. How to Interpret Resting-State fMRI: Ask Your Participants. The Journal of neuroscience 41, 1130-1141.

Greene, A.S., Gao, S., Noble, S., Scheinost, D., Constable, R.T., 2020. How Tasks Change Whole-Brain Functional Organization to Reveal Brain-Phenotype Relationships. Cell Reports 32, 108066.

Greene, A.S., Gao, S., Scheinost, D., Constable, R.T., 2018. Task-induced brain state manipulation improves prediction of individual traits. Nat Commun 9, 2807.

Habas, C., Kamdar, N., Nguyen, D., Prater, K., Beckmann, C.F., Menon, V., Greicius, M.D., 2009. Distinct cerebellar contributions to intrinsic connectivity networks. J Neurosci 29, 8586-8594.

Hamilton, J.P., Farmer, M., Fogelman, P., Gotlib, I.H., 2015. Depressive Rumination, the Default-Mode Network, and the Dark Matter of Clinical Neuroscience. Biol Psychiatry 78, 224-230.

Ichikawa, N., Lisi, G., Yahata, N., Okada, G., Takamura, M., Hashimoto, R.I., Yamada, T., Yamada, M., Suhara, T., Moriguchi, S., Mimura, M., Yoshihara, Y., Takahashi, H., Kasai, K., Kato, N., Yamawaki, S., Seymour, B., Kawato, M., Morimoto, J., Okamoto, Y., 2020. Primary functional brain connections associated with melancholic major depressive disorder and modulation by antidepressants. Sci Rep 10, 3542.

Jacob, Y., Morris, L.S., Huang, K.H., Schneider, M., Rutter, S., Verma, G., Murrough, J.W., Balchandani, P., 2020. Neural correlates of rumination in major depressive disorder: A brain network analysis. Neuroimage Clin 25, 102142.

Jo, H.J., Saad, Z.S., Simmons, W.K., Milbury, L.A., Cox, R.W., 2010. Mapping sources of correlation in resting state FMRI, with artifact detection and removal. Neuroimage 52, 571-582.

Johnson, D.P., Whisman, M.A., Corley, R.P., Hewitt, J.K., Friedman, N.P., 2014. Genetic and environmental influences on rumination and its covariation with depression. Cogn Emot 28, 1270-1286.

Jones, N.P., Fournier, J.C., Stone, L.B., 2017. Neural correlates of autobiographical problem-solving deficits associated with rumination in depression. J Affect Disord 218, 210-216.

Kuznetsova, A., Brockhoff, P.B., B., R.H., Christensen, G.E., 2017. lmerTest Package: Tests in Linear Mixed Effects Models. Journal of Statistical Software 82, 1–26.

Lenth, R.V., 2022. emmeans: Estimated Marginal Means, aka Least-Squares Means. https://CRAN.R-project.org/package=emmeans.

Lippitz, B.E., Mindus, P., Meyerson, B.A., Kihlstrom, L., Lindquist, C., 1999. Lesion topography and outcome after thermocapsulotomy or gamma knife capsulotomy for obsessive-compulsive disorder: relevance of the right hemisphere. Neurosurgery 44, 452-458; discussion 458-460.

Lois, G., Wessa, M., 2016. Differential association of default mode network connectivity and rumination in healthy individuals and remitted MDD patients. Soc Cogn Affect Neurosci 11, 1792-1801.

Lurie, D.J., Kessler, D., Bassett, D.S., Betzel, R.F., Breakspear, M., Kheilholz, S., Kucyi, A., Liegeois, R., Lindquist, M.A., McIntosh, A.R., Poldrack, R.A., Shine, J.M., Thompson, W.H., Bielczyk, N.Z., Douw, L., Kraft, D., Miller, R.L., Muthuraman, M., Pasquini, L., Razi, A., Vidaurre, D., Xie, H., Calhoun, V.D., 2020. Questions and controversies in the study of time-varying functional connectivity in resting fMRI. Netw Neurosci 4, 30-69.

Lydon-Staley, D.M., Kuehner, C., Zamoscik, V., Huffziger, S., Kirsch, P., Bassett, D.S., 2019. Repetitive negative thinking in daily life and functional connectivity among default mode, fronto-parietal, and salience networks. Transl Psychiatry 9, 234.

Makovac, E., Fagioli, S., Rae, C.L., Critchley, H.D., Ottaviani, C., 2020. Can't get it off my brain: Meta-analysis of neuroimaging studies on perseverative cognition. Psychiatry Res Neuroimaging 295, 111020.

Marek, S., Tervo-Clemmens, B., Calabro, F.J., Montez, D.F., Kay, B.P., Hatoum, A.S., Donohue, M.R., Foran, W., Miller, R.L., Hendrickson, T.J., Malone, S.M., Kandala, S., Feczko, E., Miranda-Dominguez, O., Graham, A.M., Earl, E.A., Perrone, A.J., Cordova, M., Doyle, O., Moore, L.A., Conan, G.M., Uriarte, J., Snider, K., Lynch,

B.J., Wilgenbusch, J.C., Pengo, T., Tam, A., Chen, J., Newbold, D.J., Zheng, A., Seider, N.A., Van, A.N., Metoki, A., Chauvin, R.J., Laumann, T.O., Greene, D.J., Petersen, S.E., Garavan, H., Thompson, W.K., Nichols, T.E., Yeo, B.T.T., Barch, D.M., Luna, B., Fair, D.A., Dosenbach, N.U.F., 2022. Reproducible brain-wide association studies require thousands of individuals. Nature 603, 654-660.

McCormick, E.M., Arnemann, K.L., Ito, T., Hanson, S.J., Cole, M.W., 2022. Latent functional connectivity underlying multiple brain states. Network Neuroscience 6, 570-590.

Misaki, M., Phillips, R., Zotev, V., Wong, C.K., Wurfel, B.E., Krueger, F., Feldner, M., Bodurka, J., 2018. Real-time fMRI amygdala neurofeedback positive emotional training normalized resting-state functional connectivity in combat veterans with and without PTSD: a connectome-wide investigation. Neuroimage Clin 20, 543-555.

Misaki, M., Tsuchiyagaito, A., Al Zoubi, O., Paulus, M., Bodurka, J., Tulsa, I., 2020. Connectome-wide search for functional connectivity locus associated with pathological rumination as a target for real-time fMRI neurofeedback intervention. Neuroimage Clin 26, 102244.

Montgomery, S.A., Åsberg, M., 1979. A new depression scale designed to be sensitive to change. Br J Psychiatry 134, 382-389.

Nejad, A.B., Fossati, P., Lemogne, C., 2013. Self-referential processing, rumination, and cortical midline structures in major depression. Front Hum Neurosci 7, 666.

Nolen-Hoeksema, S., Wisco, B.E., Lyubomirsky, S., 2008. Rethinking Rumination. Perspect Psychol Sci 3, 400-424.

Park, H., Kirlic, N., Kuplicki, R., Tulsa, I., Paulus, M., Guinjoan, S., 2022. Neural Processing Dysfunctions During Fear Learning but Not Reward-Related Processing Characterize Depressed Individuals With High Levels of Repetitive Negative Thinking. Biol Psychiatry Cogn Neurosci Neuroimaging.

Peters, A.T., Burkhouse, K., Feldhaus, C.C., Langenecker, S.A., Jacobs, R.H., 2016. Aberrant resting-state functional connectivity in limbic and cognitive control networks relates to depressive rumination and mindfulness: A pilot study among adolescents with a history of depression. J Affect Disord 200, 178-181.

Piguet, C., Desseilles, M., Sterpenich, V., Cojan, Y., Bertschy, G., Vuilleumier, P., 2014. Neural substrates of rumination tendency in non-depressed individuals. Biol Psychol 103, 195-202.

R Core Team, 2022. R: A Language and Environment for Statistical Computing. R Foundation for Statistical Computing, Vienna, Austria. URL https://www.R-project.org/.

Riestra, A.R., Aguilar, J., Zambito, G., Galindo y Villa, G., Barrios, F., Garcia, C., Heilman, K.M., 2011. Unilateral right anterior capsulotomy for refractory major depression with comorbid obsessive-compulsive disorder. Neurocase 17, 491-500.

Rosenberg, M.D., Finn, E.S., 2022. How to establish robust brain-behavior relationships without thousands of individuals. Nat Neurosci 25, 835-837.

Satyshur, M.D., Layden, E.A., Gowins, J.R., Buchanan, A., Gollan, J.K., 2018. Functional connectivity of reflective and brooding rumination in depressed and healthy women. Cogn Affect Behav Neurosci 18, 884-901.

Scangos, K.W., Khambhati, A.N., Daly, P.M., Makhoul, G.S., Sugrue, L.P., Zamanian, H., Liu, T.X., Rao, V.R., Sellers, K.K., Dawes, H.E., Starr, P.A., Krystal, A.D., Chang, E.F., 2021. Closed-loop neuromodulation in an individual with treatment-resistant depression. Nat Med 27, 1696-1700.

Sheehan, D.V., Lecrubier, Y., Sheehan, K.H., Amorim, P., Janavs, J., Weiller, E., Hergueta, T., Baker, R., Dunbar, G.C., 1998. The Mini-International Neuropsychiatric Interview (M.I.N.I.): the development and validation of a structured diagnostic psychiatric interview for DSM-IV and ICD-10. J Clin Psychiatry 59 Suppl 20, 22-33;quiz 34-57.

Shehzad, Z., Kelly, C., Reiss, P.T., Cameron Craddock, R., Emerson, J.W., McMahon, K., Copland, D.A., Castellanos, F.X., Milham, M.P., 2014. A multivariate distance-based analytic framework for connectome-wide association studies. Neuroimage 93 Pt 1, 74-94.

Shen, X., Finn, E.S., Scheinost, D., Rosenberg, M.D., Chun, M.M., Papademetris, X., Constable, R.T., 2017. Using connectome-based predictive modeling to predict individual behavior from brain connectivity. Nat Protoc 12, 506-518.

Shen, X., Tokoglu, F., Papademetris, X., Constable, R.T., 2013. Groupwise whole-brain parcellation from resting-state fMRI data for network node identification. Neuroimage 82, 403-415.

Stern, E.R., Eng, G.K., De Nadai, A.S., Iosifescu, D.V., Tobe, R.H., Collins, K.A., 2022. Imbalance between default mode and sensorimotor connectivity is associated with perseverative thinking in obsessive-compulsive disorder. Transl Psychiatry 12, 19.

Steward, T., Kung, P.H., Davey, C.G., Moffat, B.A., Glarin, R.K., Jamieson, A.J., Felmingham, K.L., Harrison, B.J., 2022. A thalamo-centric neural signature for restructuring negative self-beliefs. Mol Psychiatry 27, 1611-1617.

Taxali, A., Angstadt, M., Rutherford, S., Sripada, C., 2021. Boost in Test-Retest Reliability in Resting State fMRI with Predictive Modeling. Cereb Cortex 31, 2822-2833.

Tozzi, L., Zhang, X., Chesnut, M., Holt-Gosselin, B., Ramirez, C.A., Williams, L.M., 2021. Reduced functional connectivity of default mode network subsystems in depression: Meta-analytic evidence and relationship with trait rumination. Neuroimage Clin 30, 102570.

Tsuchiyagaito, A., Misaki, M., Kirlic, N., Yu, X., Sanchez, S.M., Cochran, G., Stewart, J.L., Smith, R., Fitzgerald, K.D., Rohan, M.L., Paulus, M.P., Guinjoan, S.M., 2023.

Real-Time fMRI Functional Connectivity Neurofeedback Reducing Repetitive Negative Thinking in Depression: A Double-Blind, Randomized, Sham-Controlled Proof-of-Concept Trial. Psychother Psychosom, 1-14.

Tsuchiyagaito, A., Misaki, M., Zoubi, O.A., Tulsa, I., Paulus, M., Bodurka, J., 2021. Prevent breaking bad: A proof of concept study of rebalancing the brain's rumination circuit with real-time fMRI functional connectivity neurofeedback. Hum Brain Mapp 42, 922-940.

Tsuchiyagaito, A., Sánchez, S.M., Misaki, M., Kuplicki, R., Park, H., Paulus, M.P., Guinjoan, S.M., 2022. Intensity of repetitive negative thinking in depression is associated with greater functional connectivity between semantic processing and emotion regulation areas. Psychol Med, 1-12.

Watkins, E.R., Roberts, H., 2020. Reflecting on rumination: Consequences, causes, mechanisms and treatment of rumination. Behav Res Ther 127, 103573.

Winkler, A.M., Ridgway, G.R., Webster, M.A., Smith, S.M., Nichols, T.E., 2014. Permutation inference for the general linear model. Neuroimage 92, 381-397.

Wise, T., Marwood, L., Perkins, A.M., Herane-Vives, A., Joules, R., Lythgoe, D.J., Luh, W.M., Williams, S.C.R., Young, A.H., Cleare, A.J., Arnone, D., 2017. Instability of default mode network connectivity in major depression: a two-sample confirmation study. Transl Psychiatry 7, e1105.

Yan, C.G., Chen, X., Li, L., Castellanos, F.X., Bai, T.J., Bo, Q.J., Cao, J., Chen, G.M., Chen, N.X., Chen, W., Cheng, C., Cheng, Y.Q., Cui, X.L., Duan, J., Fang, Y.R., Gong, Q.Y., Guo, W.B., Hou, Z.H., Hu, L., Kuang, L., Li, F., Li, K.M., Li, T., Liu, Y.S., Liu, Z.N., Long, Y.C., Luo, Q.H., Meng, H.Q., Peng, D.H., Qiu, H.T., Qiu, J., Shen, Y.D., Shi, Y.S., Wang, C.Y., Wang, F., Wang, K., Wang, L., Wang, X., Wang, Y., Wu, X.P., Wu, X.R., Xie, C.M., Xie, G.R., Xie, H.Y., Xie, P., Xu, X.F., Yang, H., Yang, J., Yao, J.S., Yao, S.Q., Yin, Y.Y., Yuan, Y.G., Zhang, A.X., Zhang, H., Zhang, K.R., Zhang, L., Zhang, Z.J., Zhou, R.B., Zhou, Y.T., Zhu, J.J., Zou, C.J., Si, T.M., Zuo, X.N., Zhao, J.P., Zang, Y.F., 2019. Reduced default mode network functional connectivity in patients with recurrent major depressive disorder. Proc Natl Acad Sci U S A 116, 9078-9083.

Yang, M.H., Guo, Z.P., Lv, X.Y., Zhang, Z.Q., Wang, W.D., Wang, J., Hong, L., Lin, Y.N., Liu, C.H., 2022. BMRMI Reduces Depressive Rumination Possibly through Improving Abnormal FC of Dorsal ACC. Neural Plast 2022, 8068988.

Zhang, J., Kucyi, A., Raya, J., Nielsen, A.N., Nomi, J.S., Damoiseaux, J.S., Greene, D.J., Horovitz, S.G., Uddin, L.Q., Whitfield-Gabrieli, S., 2021. What have we really learned from functional connectivity in clinical populations? Neuroimage 242, 118466.

Zhang, R., Kranz, G.S., Zou, W., Deng, Y., Huang, X., Lin, K., Lee, T.M.C., 2020. Rumination network dysfunction in major depression: A brain connectome study. Prog Neuropsychopharmacol Biol Psychiatry 98, 109819.

Zhang, R., Tam, S.T.S., Wong, N.M.L., Wu, J., Tao, J., Chen, L., Lin, K., Lee, T.M.C., 2022. Aberrant functional metastability and structural connectivity are associated with rumination in individuals with major depressive disorder. Neuroimage Clin 33, 102916.

Zhu, X., Zhu, Q., Shen, H., Liao, W., Yuan, F., 2017. Rumination and Default Mode Network Subsystems Connectivity in First-episode, Drug-Naive Young Patients with Major Depressive Disorder. Sci Rep 7, 43105.